Proceedings of the 7th International Conference on Asian and Pacific Coasts (APAC 2013) Bali, Indonesia, September 24-26, 2013

CHANGES IN TSUNAMI BEHAVIOR IN THE HARBOR ZONE DUE TO DEVELOPMENT OF WIND-WAVE BREAKWATERS

T. Kikuchi [1], T. Yamashita [2], M. Hara[3] and T. Komaguchi [4]

ABSTRACT: Expansion of port facilities, such as extension and new construction of the harbor breakwaters and landfill, greatly changes the distribution characteristics of the tsunami height in the harbor zone. As harbor breakwaters are designed to defend the invasion of wind waves, its external force is small in the shallow water and large in deep water. On the other hand, tsunami height becomes higher in the shallow water. Such a difference of external force distribution between wind-waves and tsunamis, increases the destruction possibility of harbor breakwaters in the shallow region at the tsunami event. The extension of the harbor breakwaters attenuates the tsunami energy inside the port. However, outside the breakwaters, the tsunami energy is captured by breakwater and concentrated in the base portion of breakwater leaving a high possibility of breakwater destruction.
Once the breakwater is destroyed, the concentrated tsunami intrudes into the port resulting in the serious tsunami damages. In this way, the tsunami behavior in the port area is largely affected by the shape of harbor breakwater and its resilience tsunami forces. This paper conducted a numerical analysis of tsunami propagation in Akita Harbor considering effects of harbor structure, tsunami overtopping, breakwater failures, and tsunami inundation onto the land to clarify the relation between harbor structure and tsunami propagation. The earthquake was assumed to occur along the plate boundary of the north-eastern margin of the Japan Sea.

Keywords: Tsunami propagation and deformation, run-up, harbor breakwaters, Nihonkai Chubu Earthquake

INTRODUCTION

The tsunami caused by the Nihonkai Chubu Earthquake (the Sea of Japan Earthquake) in 1983 flooded the low-lying area of northern Akita harbor, and scattered wave-absorbing blocks several 10m from the coast. On the other hand, flood damage in the canal of the Akita harbor has not occurred. The reason for this is because breakwater of the Akita harbor attenuated sufficiently tsunami energy to reduce the tsunami height flowing into the harbor canal. Breakwater of Akita harbor has been extended up to about 1.5km off the coast in the current 20 years. The north breakwater has also been newly installed and harbor facilities expanded by landfill. After the harbor terrain conditions (buildings and structures) have been changed, the current topographical conditions seem to be more safety in the harbor canal against intrusion of tsunami than the conditions in 1983. However, it is also possible to consider that the breakwater extension increases the risk of changing the concentration characteristics of tsunami height outside the harbor, resulting in the tremendous high tsunami energy at the base of breakwater. If the old southern breakwater (base of the breakwater) of Akita harbor is destroyed by the tsunami, concentrated water mass here may also be possible to flow into the canal to occur the inundation of harbor facilities.

In this study, as an example of tsunami propagation and deformation in the Japan Sea, numerical analysis of tsunami behavior near the large-scale harbor breakwater of Akita harbor is conducted. The followings will be examined, tsunami propagation around the breakwater and flooding onto the land of port facilities, to make clear the tsunami behavior associated with the extension of the harbor breakwater and the changes in the disaster morphology caused by tsunami.

SUBMARINE EARTHQUAKE IN JAPAN SEA

The tsunami propagation simulation in the open ocean was carried out targeting the entire Sea of Japan. The tsunami behavior affected by the harbor structures and tsunami run-up onto the land have also been computed. Target sub-marine earthquakes in this study are the Central Japan Sea earthquake occurred in 1983 (Nihonkai Chubu) and a Northern Off Sado Island earthquake (Sadohoppo-oki) that is anticipated its

[1] Idemitsu Kosan Co.,Ltd., Makuhari Techno Garden, Chiba, 261-8501, JAPAN
[2] IDEC, Hiroshima University, 1-5-1 Kagamiyama, Higashi-Hiroshima, 739-8529, JAPAN
[3] Idemitsu Kosan Co., Ltd., Makuhari Techno Garden, Chiba, 261-8501, JAPAN
[4] Blue Wave Institute of Technology, Taito-ku, Motoasakusa 1-17-15, Tokyo, 111-0041, JAPAN

occurrence along the Eastern Margin of the Japan Sea. These earthquakes are part of tsunami-generated submarine earthquakes continuously occurred in the Sea of Japan in 20th century as shown in Fig.1. Those are Shakotanhanto-oki Earthquake (1940) in Off North Hokkaido Region, Niigata Earthquake (1964) in Off Niigata Region, Nihonkai Chubu Earthquake (1983) in Off West Aomori Region, and Hokkaido Nansei-oki Earthquake(1993) in North South Hokkaido Region.

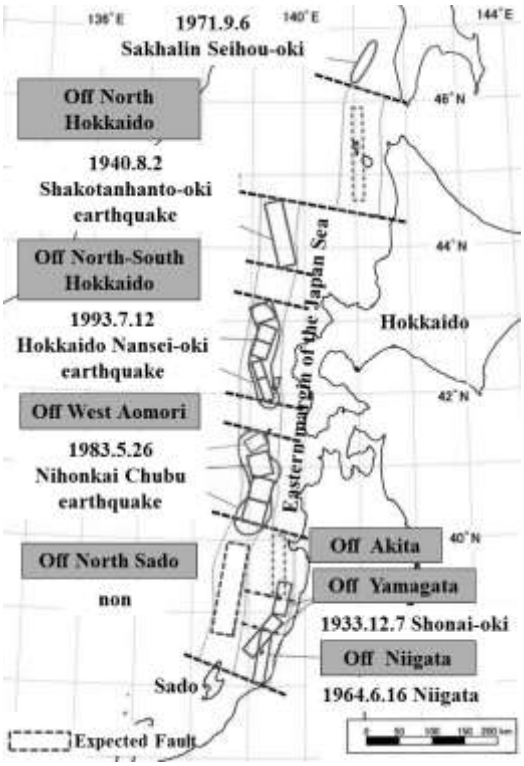

Fig. 1 Tsunami-generated submarine earthquakes occurred in the Sea of Japan in 20th century.

Nihonkai Chubu Earthquake in 1983 (Baseline Tsunami Propagation Simulation)

Nihonkai-Chubu earthquake occurred in 1983 had a magnitude of Mw=7.8 on the moment magnitude scale. Its highest tsunami height exceeded 10m in some areas. Fig.2 shows the observed tsunami height along the Japan Sea. In this study reanalysis of tsunami caused by 1983 Nihonkai-Chubu earthquake is the baseline simulation to verify the simulation code. The seismic fault model employed in this study is Aida's fault model (Aida, 1984) of which parameters are shown in Table 1 as "Nihonkai Chubu 1983". Another seismic fault model for Sadohoppo-oki earthquake is also shown in the table. Enhanced Nihonkai Chubu and Enhanced Sadohoppo-oki earthquakes are defined as fault models of which displacement u(m) are two-times larger than original earthquake. Fig.3 shows the definition of seismic fault model parameters.

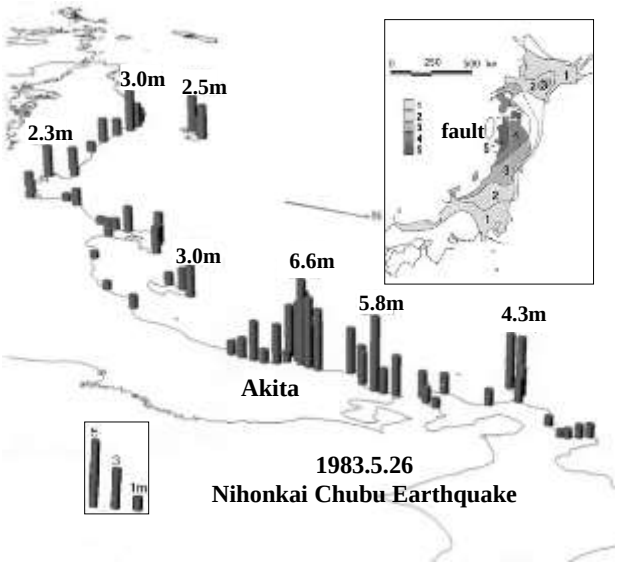

Fig. 2 Tsunami height distribution of 1983 Nihinkai Chubu earthquake.

Table 1 Seismic fault model parameters used.

Earthquake	M_w	S (km^2)	L (km)	W (km)	u (m)	D (km)	ϕ (deg)	δ (deg)	λ (deg)
Nihonkai Chubu 1983 (real earthquake)	7.74	1200	40	30	7.6	2	22	40	90
		1800	60	30	3.05	3	355	25	80
Enhanced Nihonkai Chubu (virtual earthquake)	7.94	1200	40	30	15.2	2	22	40	90
		1800	60	30	6.1	3	355	25	80
Sadohoppo-oki (virtual earthquake)	7.81	4760	140	34	3.86	1	190	30	90
Enhanced Sadohoppo-oki (virtual earthquake)	8.01	4760	140	34	7.72	1	190	30	90

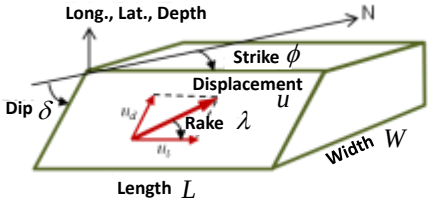

Fig. 3 Definition of seismic fault model.

TSUNAMI SIMULTION IN JAPAN SEA

The horizontally two dimensional simulation code developed by Goto & Ogawa (1985) was used to integrate the nonlinear long wave equations. In order to perform tsunami simulation with high accuracy five-level nesting system was employed as; Domain-1: The Sea of Japan waters, including the seismic zone, its mesh size is 1,350 m, Domain-2: Sado Island waters, its mesh size is 450m, Domain-3: Off Akita-1, 150m, Domain-4: Off Akita-2, 50m, and Domain-5: Akita Port Area, DS=50/3 m. Fig.4 shows a computational domains

Using the M7000 series digital bathymetry data of the Japan Coast Guard Hydrographic Department and GEBCO-30, the water depth in each computational

domain were generated in the coordinate system of UTM53.

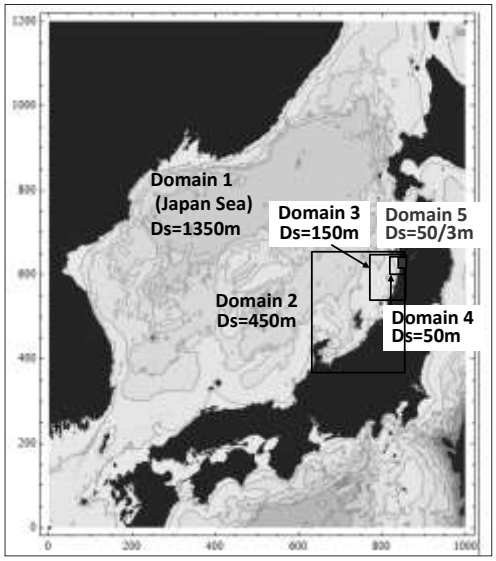

Fig. 4 Computational domains.

Fig. 5 shows a tsunami propagation generated by Enhanced Nihonkai Chubu Earthquake in the Japan Sea up to 120min after the shock.

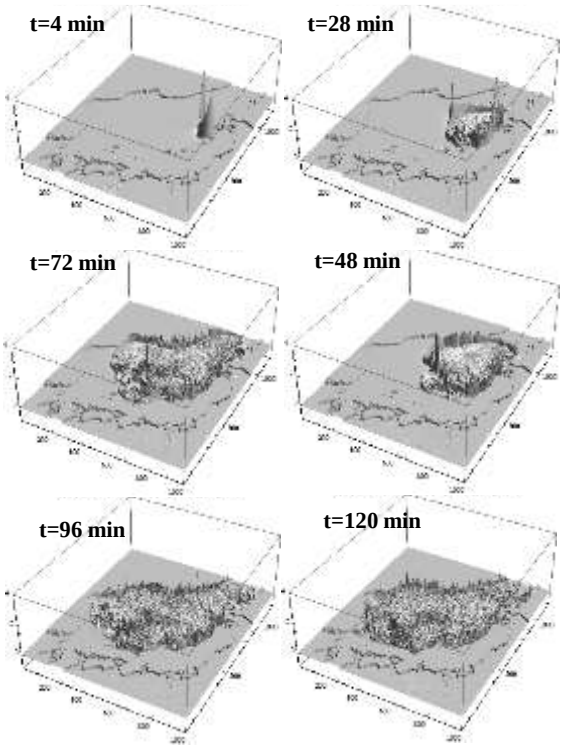

Fig. 5 Tsunami propagation generated by Enhanced Nihonkai Chubu Earthquake.

Fig.6 depicts the tsunami propagation and deformation in the Domain-2, Sado Island Waters every 10min after the shock of Enhanced Nihonkai Chubu Earthquake which is a virtual earthquake that has two times larger displacement of 1983 Nihonkai Chubu Earthquake.

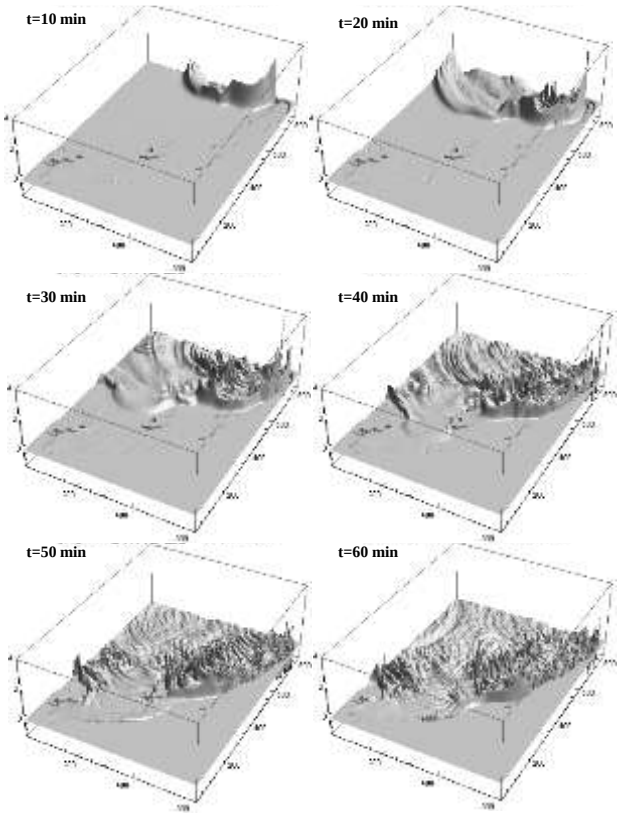

Fig. 6 Tsunami propagation and deformation of Enhanced Nihonkai Chubu Earthquake in the Domain-2.

Model Verification by 1983 Nihonkai Chubu

Fig.7 shows a comparison of the computed tsunami height of 1983 Nihonkai Chubu earthquake in the computational Domains-1 and -2 (in red line) and the observed height (in blue bars) at monitoring points along the coasts of Hokkaido, Tohoku and Hokuriku. Tsunami height of 1983 Nihonkai Chubu Earthquake are higher than 2m in south Hokkaido (highest at Fukaura) and Aomori-Akita Prefectures (Tohoku) except the southern part of the Oga Peninsula (north of Akita). It can be seen that the computed tsunami heights reproduced observed data with sufficient accuracy along the Japan Sea. The observed tsunami heights in the figure are cited from Watanabe (1998) and the tsunami traces database of Tohoku University.

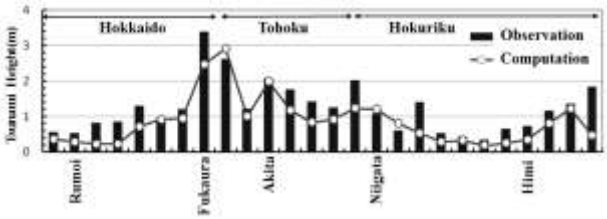

Fig. 7 Comparison of the computed tsunami height and the observed data at monitoring points from Hokkaido to Hokuriku (1983 Nihonkai Chubu Earthquake).

TSUNAMI BEHAVIOR NEAR BREAKWATERS OF AKIT HARBOR

Linea Structure and Topography near Akita Harbor

For the land topography creation to simulate tsunami run-up to the land, 5m DEM of base map information of national GSI was used. For linear structures around Akita Harbor, a quay and embankment data (location and crown heights) were extracted from the plan view of Akita harbor (Fig.8) .

Fig.9 shows the created topography of Akita harbor which will be used for the simulation of tsunami behavior near the breakwater and inundation onto land.

Fig. 8 A plan view of Akita harbor and river bank data of the Monobegawa river.

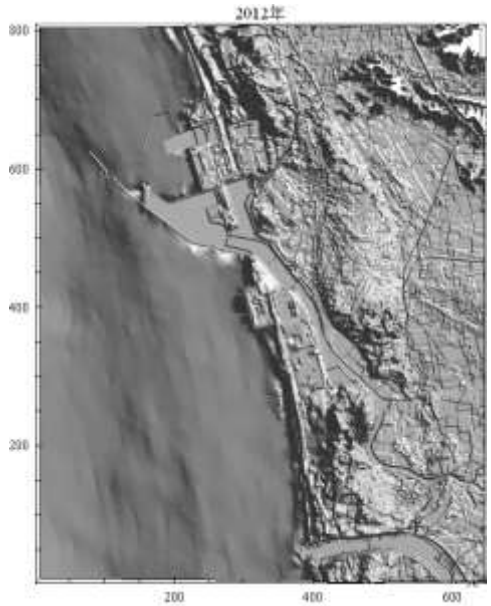

Fig. 9 The topography of Akita harbor in 2012.

Computational Set-up

For the computation of tsunami behavior in the Akita harbor area (Domain-5), 16 cases were set up with 4 cases of Earthquake and 4 cases of harbor structures. Table 2 shows 16 computational cases. Three cases for breakwaters in 1983, 2012 (real) and the no breakwater case (virtual) and one partial breakwater failure case due to tsunami concentration at the root of harbor breakwater.

Table 2 Computational set-up (4x4 cases)

Earthquake		Structure conditions
Nihonkai Chubu 1983	×	Breakwater 1983
Enhanced Nihonkai Chubu		Breakwater 2012
Enhanced Nihonkai Chubu + Sadohoppo-oki		Breakwater Partial failure
Enhanced Nihonkai Chubu + Enhanced Sadohoppo-oki		No Breakwater

Fig. 10 shows the topography, structures and output points of computed water elevation inside and outside the Akita harbor. Points 91-98 are on the land to detect tsunami inundation. Points 81-88 are inside the Akita harbor to show the tsunami behavior in the port. Points 61-64 are outside the harbor to detect the concentration of tsunami at the root of breakwater.

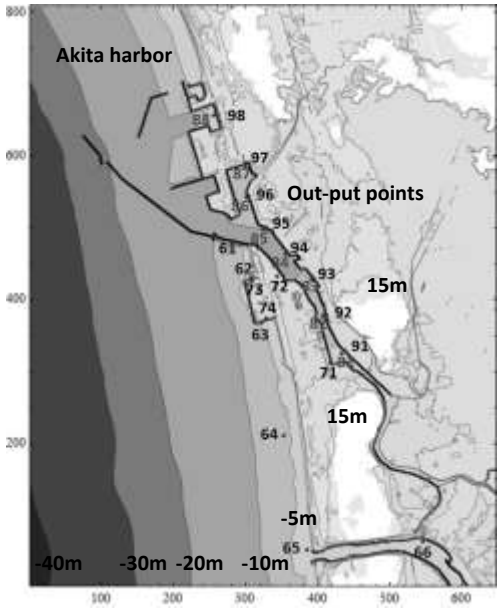

Fig. 10 Topography, structures and output points in computational Domain-5 (Akita harbor).

Simulation Results of 1983 Nihonkai Chubu Earthquake (Real Case)

The computational results of tsunami propagation in the Domains 1, 2, 3 and 4 are linked to Domain-5 in which the moving boundary condition (wet-dry condition) are set up to simulate tsunami run up onto the land. Reproduction of tsunami behavior of 1983

Nihonkai Chubu earthquake was conducted to make sure the observed facts "The tsunami caused by the 1983 Nihonkai Chubu Earthquake flooded the low-lying area of northern Akita harbor."

Fig.11 shows the maximum tsunami height (5.65m at the root of breakwater) and inundation depth of tsunami caused by 1983 Nihinkai Chubu. Fig.12 shows the maximum velocity distribution.

However, from the figure, the flooding area is not recognized in the Akita harbor except root of breakwater.

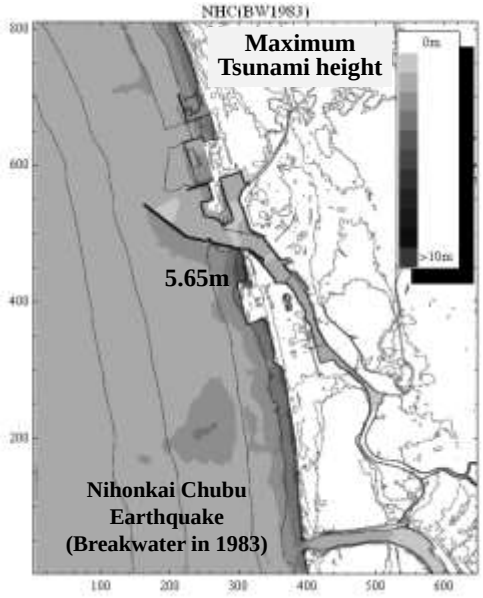

Fig. 11 The maximum tsunami height and inundation depth of 1983 Nihonkai Chubu earthquake.

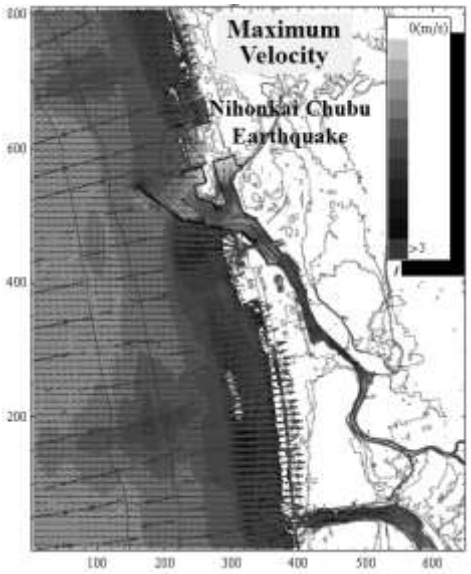

Fig. 12 The maximum velocity distribution of 1983 Nihonkai Chubu earthquake tsunami.

Fig. 13 left shows the maximum tsunami height and inundation depth when no breakwater conditions (no protection) are assumed. The right figure shows the difference in maximum water elevation between real case and no breakwater assumption case. Blue area indicates the increase of water level and red area shows the reduced water level (effect of breakwater for tsunami height reduction). If there is no breakwater, a slight inundation occurred in the inner area of the harbor that is called the harbor canal.

Computed water elevation changes are shown in Fig.14 at the out-put points in the sea (81-88, 61-66). It is shown that the maximum elevations are the first wave at about 37min after the shock. Harbor oscillation occurred at the point 81, the end of harbor canal.

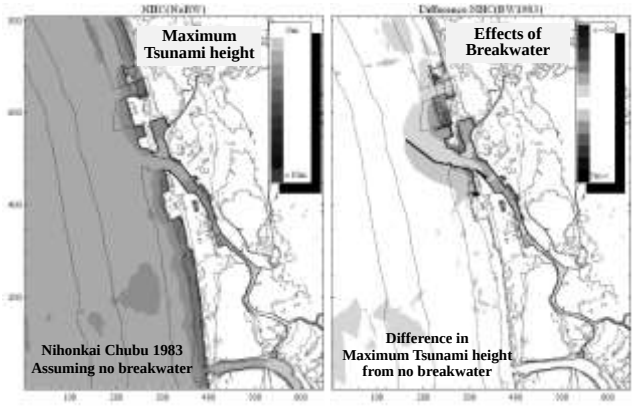

Fig. 13 Maximum tsunami height and inundation depth for no breakwater condition (left) and water level difference between with and without breakwater(right).

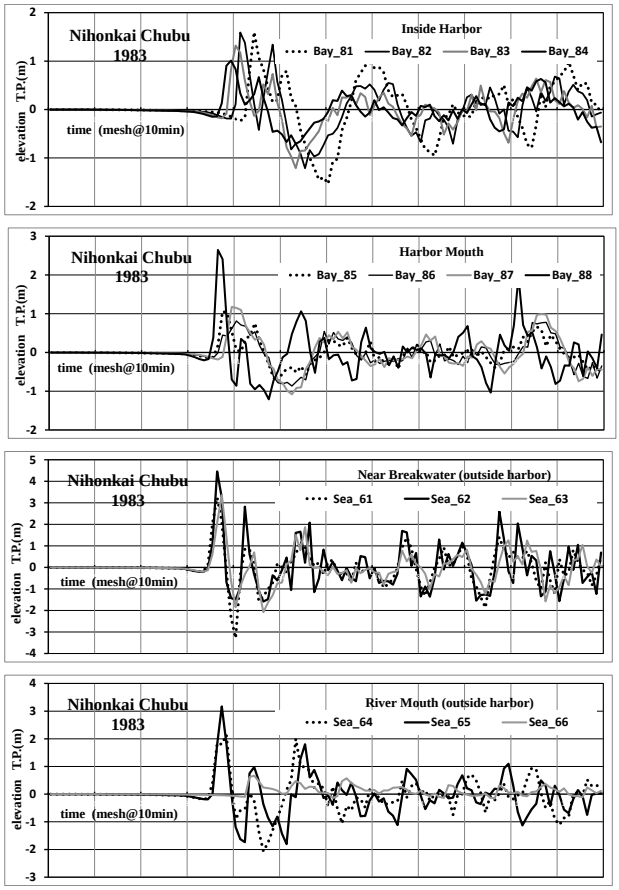

Fig. 14 Computed water elevation changes at the out-put points, 81-88 and 61-66.

Simulation Results of Virtual Earthquake Cases

In the case of 1983 Nihonkai Chubu Earthquake, the maxmimum tsunami height was 5.65m at the root of breakwate outside the harbor. This tsunami did not cause serious inundation nor brwakwater failure.

Expansion of port facilities, such as extension and new construction of the harbor breakwaters and landfill, greatly changes the distribution characteristics of the tsunami height in the harbor zone.

Conducting the tsunami simulation caused by virtual sever earthquakes, Enhanced Nihonkai Chubu (EHNC) and Sadohoppo-oki (SHO) Earthquake and their simultaneous occurrence cases, tsunami concentration characteristics near the harbor breakwater are examined in this chapter. Fig.15 shows the maximum tsunami height and inundation depth of the virtual earthquake tsunamis.

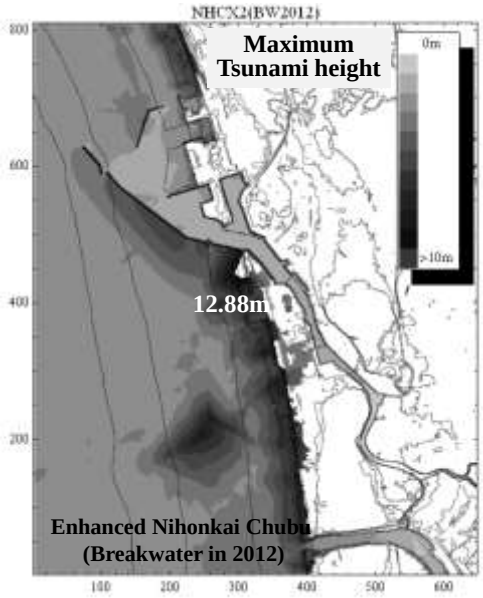

(a) Enhanced Nihonkai Chubu earthquake.

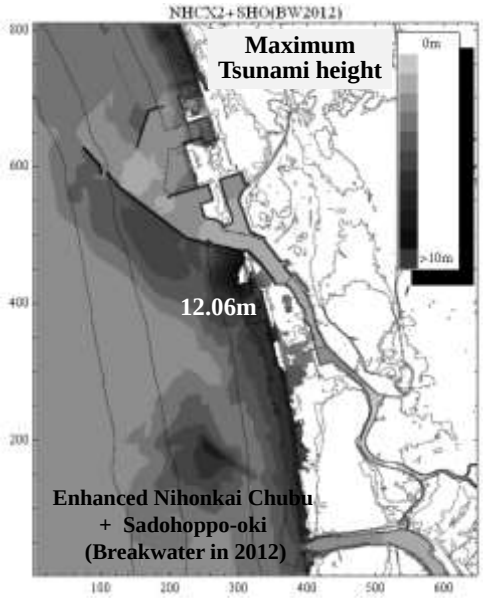

(b) Coincidence of EHNC and SHO earthquakes.

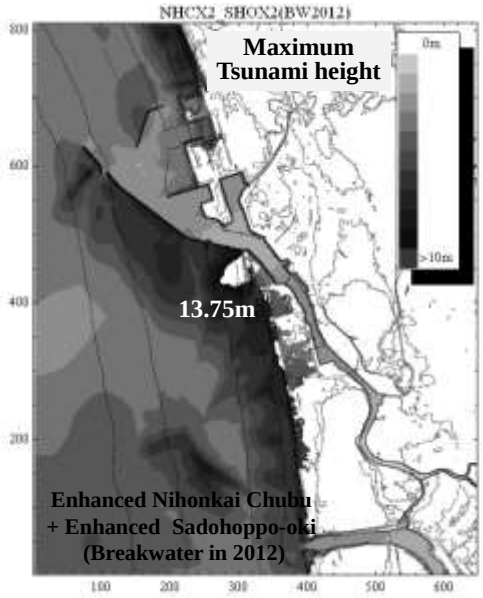

(c) Coincidence of EHNC and Enhanced Sadohoppo-oki earthquakes.

Fig.15 The maximum tsunami height and inundation depth of virtual earthquake tsunami.

From the results of virtual earthquake cases, it was made clear that the maximum tsunami height at the root of breakwater became tremendous high values, such as 12.88m for EHNC, 12.06m for coincidence of EHNC and SHO earthquakes, 13.75m for coincidence of EHNC and Enhanced Sadohoppo-oki (EHSHO) earthquakes. These are extremely high compared with 5.65m of 1983 Nihonkai Chubu. It may cause breakwater faulure at its root area.

Fig.16 shows the maximum tsunami heights of EHNC and coincidence of EHNC and ESHO earthquake under the breakwater condition in 1983. By comparing Fig.15 (a) , (c) and Fig.16, the followings are understood. The increases in the maximum tsunami height from breakwater conditions in 1983 and 2012 are 50cm (+3.8％) for EHNC, 70cm (+5.0％) for coincident earthquakes of EHNC and SHO.

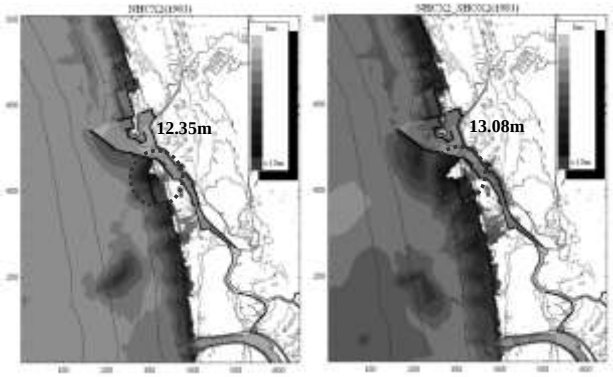

Fig.16 maximum tsunami heights of EHNC and coincidence of EHNC and EHSHO earthquake under the breakwater condition in 1983

Simulation Results of Breakwater Failure

As harbor breakwaters are designed to defend the invasion of wind waves, its external force is small in the shallow water and large in deep water. On the other hand, tsunami height becomes higher in the shallow water. Such a difference of external force distribution between wind-waves and tsunamis, increases the destruction possibility of harbor breakwaters in the shallow region at the tsunami event. The extension of the harbor breakwaters attenuates the tsunami energy inside the port. However, outside the breakwaters, the tsunami energy is captured by breakwater and concentrated in the root of breakwater leaving a high possibility of breakwater destruction.

As mentioned in Fig.15, the tsunami heights of virtual earthquakes became more than 12 to 13m high at the root of breakwater. Since the crown height of the breakwater here is 6.7m from MSL, a part of breakwater may be destructed due to overflow of water.

The following part of the paper indicats the results of numerical analysis of tsunami propagation in Akita Harbor considering effects of tsunami overtopping, breakwater failures, and tsunami inundation onto the land to clarify the relation between harbor structure and tsunami propagation.

Fig.17 shows the maximum tsunami heights with and without failure of the initial breakwater that was built in the first (upper) and their differences near the root of harbor breakwater (lower) for each virtual earthquake.

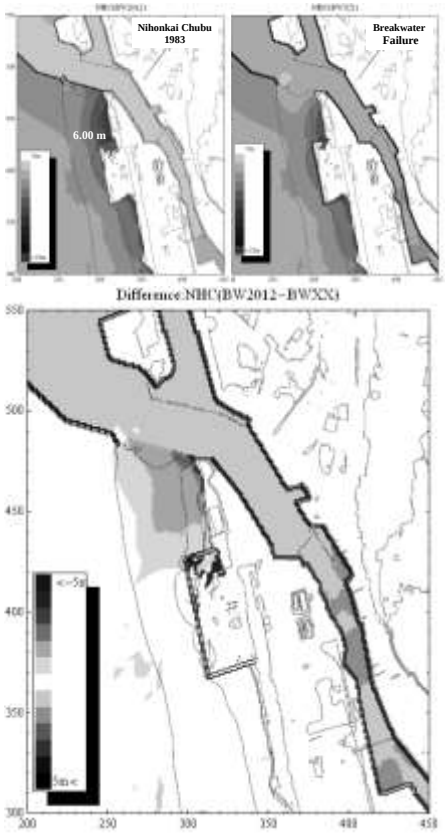

(a) 1983 Nihonkai Chubu earthquake

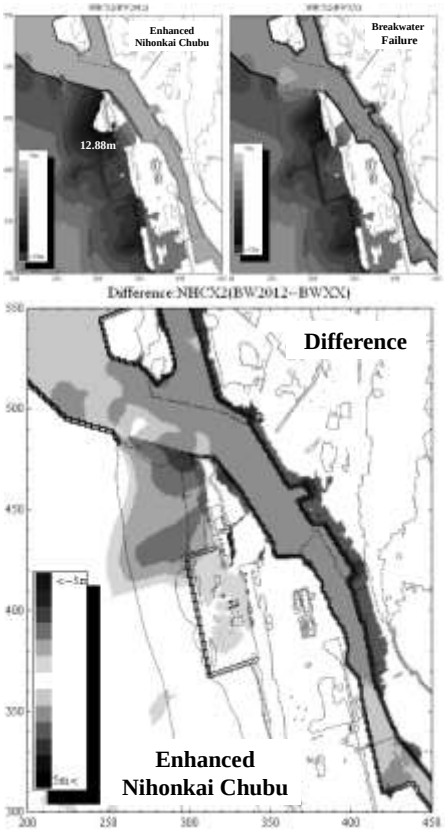

(b) Enhanced Nihonkai Chubu earthquake

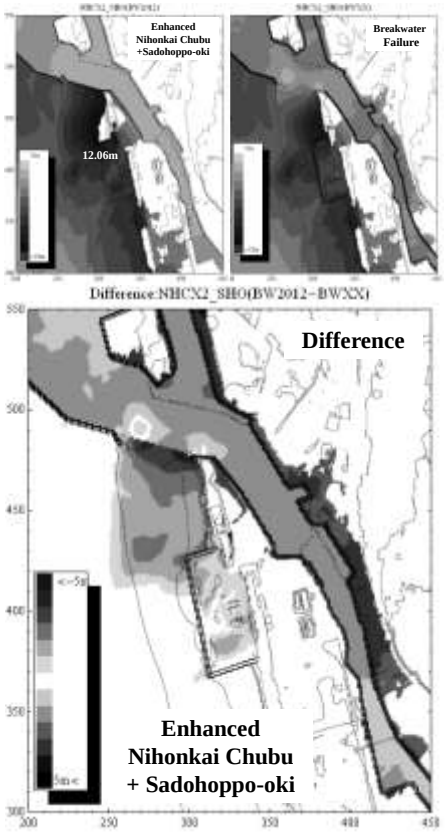

(c) Coincidence of Enhanced Nihonkai Chubu and Sadohoppo-oki earthquakes.

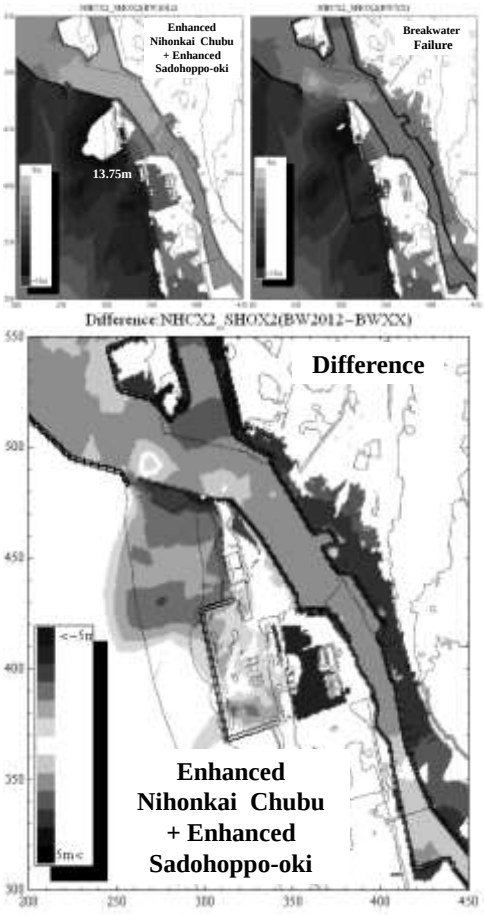

(d) Coincidence of Enhanced Nihonkai Chubu and Enhanced Sadohoppo-oki earthquakes.

Fig.17 Maximum tsunami heights with and without failure of the initial breakwater (upper) and their differences near the root of harbor breakwater (lower).

From the output shown in Fig.17, the following things are made clear as the effects of breakwater failure.
1) If 1983 Nihonkai Chubu earthquake occurred under the breakwater condition in 2012, maximum tsunami height increases to 6.00m from 5.65m (under 1983 breakwater condition). When 6.00m tsunami can make breakwater failure, the amount of maximum tsunami height inside the harbor canal ranges 1-2m which is lower level than seawall (see Fig.17(a)).
2) In the case of ENHC earthquake shown in Fig.17(b), the maximum height reaches 12.88m at the root of breakwater that is higher than 12.06m of the coincidence case of EHNC and SHO earthquakes (Fig.17(c)). It can be recognized that inundation may occur along the harbor canal with the level of around 4m above the MSL (inundation depth is 2m).
3) The case of coincidence of EHNC and SHO earthquakes, increase in water level inside the harbor canal becames larger than the case of ENHC earthquake. Wider inundation area is projected as shown in Fig.17(c).
4) The worst case of coincidence of EHNC and EHSHO earthquakes indicates the possibility of seriou inundation in Akita City with the maximum water level of 5m. However inundation area in the south of harbor may shrink as shown in Fig.17(d).

CONCLUSIONS

The conducted numerical simulations of tsunami propagation in the Japan Sea were conducted assuming 4 submarine earthquakes along the plate boundary of the north-eastern margin of the Japan Sea.

Using a five-level nesting, the detail simulations of tsunami propagation and deformation including run up in Akita harbor were also conducted. The major results of this study are summarized as follows;

1) The tsunami propagation model was verified by the reproduction of 1983 Nihonkai Chubu earthquake tsunami along the Japan Sea.
2) The reproduction of 1983 Nihonkai Chubu earthquake tsunami in Akita harbor showed the maximum tsunami height was 5.65m at the root of the initial breakwater.
3) Due to the extension of the breakwater accompanied by harbor development, tsunami energy was integrated into a root of breakwater resulting in extremely high wave height. The increases in the maximum tsunami height from breakwater conditions in 1983 and 2012 are 50cm (+3.8%) for Enhanced Nihonkai Chubu, 70cm (+5.0 %) for coincident earthquakes of Enhanced Nihonkai Chubu and Enhanced Sadohoppo-oki.
4) The extension of the harbor breakwaters causes the tsunami energy concentration at the root of breakwater. In the case of Akita harbor, the seriou inundation may occur when the initial breakwater is destroyed. The maximum water level of the inundation reaches about 5m above MSL.

ACKNOWLEDGEMENTS

Dr. Y. Isozaki, Blue Wave Institute of Technology, kindly contributed to this research with creating the land topography data in Akita Harbor.

REFERENCES

Aida, I (1984). A Source Model of the Tsunami Accompanying the 1983 Nihonkai-Chubu Earthquake, Bull. of Eartq. Res. Ins., Uni. Tokyo, Vol. 59: 93-104.

Watanabe, H. (1998). Japan Tsunami Damage Overview (second edition), University of Tokyo Press, 238p.

Goto, C. and Y. Ogawa (1982). Numerical simulation method of tsunami propagation using leap-flog scheme, Civil Engineering Department, Tohoku University, 52p.